Anisotropic domain evolution in epitaxial Fe/GaAs(001) wires

U. Ebels,* A. O. Adeyeye, M. Gester,† R. P. Cowburn, C. Daboo, and J. A. C. Bland
Cavendish Laboratory, University of Cambridge, Madingley Road, Cambridge CB3 OHE, United Kingdom
(Received 24 January 1997)

The magnetization reversal in in-plane magnetized epitaxial Fe/GaAs(001) wire elements with dimensions of 15 μm (width w)$\times$500 μm (length l)$\times$300 Å (Thickness t) has been studied by scanning Kerr microscopy and Kerr magnetometry. The two-jump switching process is observed which is characteristic for the magnetization reversal in continuous epitaxial Fe(001) films with fourfold in-plane anisotropy. However, in contrast to the continuous film, the domain nucleation and growth processes which mediate the irreversible magnetization jumps at the two critical fields, H_{c1} and H_{c2} are found to be determined by the orientation of the applied field with respect to the long and the short wire axis. This anisotropy in the domain evolution is a result of the combined effects of *local* edge dipolar fields, the fourfold magnetocrystalline anisotropy as well as the finite and anisotropic lateral extensions of the wires. Due to the large aspect ratio of l/w, the boundaries of the long and short wire edges restrict the domain expansion differently. Consequently, this ''shape'' anisotropy in the domain evolution contrasts with the conventional shape anisotropy associated with *macroscopic* (average) demagnetization fields. [S0163-1829(97)04334-8]

I. INTRODUCTION

Low-dimensional magnetism has been of central interest in the past decade stimulated by the discovery of phenomena in ultrathin films and multilayers and the potential application of these thin-film systems for magnetic storage media and sensor technology.[1] Starting from these quasi-two-dimensional thin-film systems, interest is now shifting towards studying smaller and smaller physical dimensions achieved by laterally constraining the thin films to micron and nanometer sized wire and dot structures.[2,3] On reducing the sample sizes to dimensions comparable to relevant physical length scales, such as the domain-wall width or the exchange length, questions arise concerning the existence of a true single-domain state, the magnetic switching characteristics as well as the stability of the domain state.[4] A broad understanding of all effects which influence the magnetization state in small magnetic elements and in particular those effects associated with the sample edges, is therefore of great relevance. More generally, the importance of local symmetry-breaking structures such as edge or step edges on the magnetization reversal process has been recently pointed out theoretically.[5]

Interest in magnetization processes in small magnetic film elements is not entirely new. In the past, the study of micron and submicron sized in-plane magnetized small film elements of Permalloy has been of great significance.[6,7] Knowledge of the domain and domain-wall structure is crucial in understanding the noise properties of these elements in their application as read heads in magnetic recording.[8] While many studies were performed for these Permalloy film elements, characterized by a very small magnetic anisotropy, only a few investigations have been made for materials with strong magnetic anisotropies.[9,10] This paper focuses on the in-plane magnetization processes in flat wires fabricated from *epitaxial* Fe/GaAs(001) thin films and contrasts the developing domain structures with those in Permalloy small film elements. The pronounced difference between the two materials is the more than 1 order of magnitude larger value of the magnetic anisotropy in Fe with an anisotropy field of $H_{K_1}=2K_1/M_s=550$ Oe as compared to Permalloy with $H_{K_u}\cong 10$ Oe. Here, K_1 and K_u represent the cubic and the uniaxial anisotropy constants for Fe and Permalloy, respectively, and M_S denotes the saturation magnetization.

In addition, the epitaxial nature of the Fe system has the advantage of a well-defined magnetocrystalline anisotropy superposed by a controllable interface-induced anisotropy resulting in characteristic magnetization reversal processes as a function of an externally applied field. These anisotropy characteristics as well as the corresponding magnetization reversal processes have been widely studied for continuous epitaxial Fe thin films evaporated onto substrates such as GaAs(001),[11–13] W(001),[14] and Ag(001).[15] Bulk Fe has a cubic magnetocrystalline anisotropy K_1 which gives rise to a fourfold in-plane anisotropy in Fe(001) thin films, with the easy axis (EA) oriented parallel to the $\langle 100\rangle$ direction and the hard axis (HA) parallel to the $\langle 110\rangle$ direction. This fourfold in-plane magnetocrystalline anisotropy leads to the typical two-jump switching[12] associated with two critical fields H_{c1} and H_{c2} for the reversal of the magnetization in an applied field. The energetics of this two-jump switching process for continuous Fe/GaAs(001) thin films are discussed in Ref. 2. In the present study the investigations of the magnetization reversal processes in continuous Fe/GaAs(001) films are extended to micron-sized Fe/GaAs(001) wires where the combined effects of *local* dipolar fields in the vicinity of the wire edges, as well as the anisotropic and finite extensions, modify the evolution of the magnetic domains which develop at the critical fields H_{c1} and H_{c2}. Understanding of this magnetization reversal will be of importance for the recently proposed magnetoelectronic devices such as microwave,[16] current injection, and MRAM devices[16,17] which exploit the switching characteristics of these epitaxial magnetic materials deposited on semiconductor substrates.

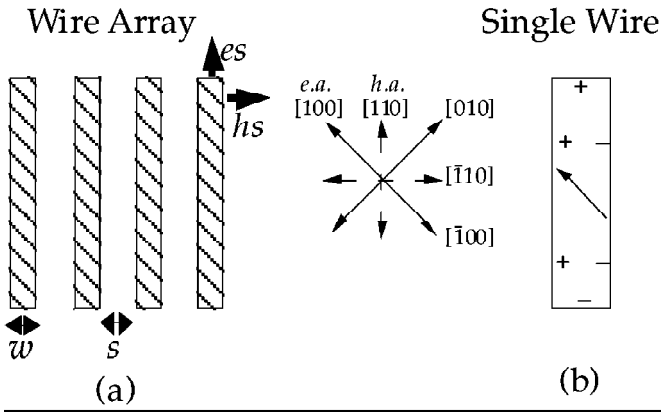

FIG. 1. (a) Schematic showing the arrangement of the wire array with wires of width w and separation s between individual wires. (b) Schematic showing a single wire, the orientation of the magnetization when aligned parallel to the easy axis [100] and the resulting charges along the wire edges.

II. EXPERIMENT

The continuous 300-Å-thick Fe/GaAs(001) film, from which the wire structures were patterned, was prepared in ultrahigh vacuum (UHV) by electron beam evaporation.[13] The base pressure during growth was kept at 10^{-9} mbar and the growth rate was 1 Å/min. The wire structures were fabricated by optical lithography and ion beam etching.[18] In order to ascertain that the observed domain structures are reproducible and not due to local film inhomogeneities, an array consisting of evenly spaced wires was patterned as schematically shown in Fig. 1(a). The total number of wires in an array amounts to 20. A total of 9 arrays were fabricated with identical wire width of value $w=15$ μm but different spacing s between the wires ranging from $s=6$ to 22 μm. The dimensions of the individual wires are 15 μm (width w) (length l)$\times 300$ Å (thickness t). This choice and, in particular, the one of the wire width $w=15$ μm was guided by the use of an optical domain imaging microscope. The scanning Kerr microscope used for the present study has a resolution of 1.5 μm and thus dimensions of at least 5–10 μm are required in order to resolve details of the domain structure. Due to the cubic magnetocrystalline anisotropy, two relative orientations between the wire edges and the anisotropy axes are of interest. For the present study, the orientation of the wire edges was chosen such that both wire axes are aligned parallel to the cubic hard axes ($\langle 110\rangle$) within an accuracy of $\pm 5°$, see Fig. 1(b).

Spatially averaged hysteresis loops as well as images of the magnetic domain structure are presented for different field orientations and at the two critical fields H_{c1} and H_{c2}. The hysteresis loops were recorded with a conventional magnetooptic Kerr effect (MOKE) magnetometer (0.5 mm spot size) and the domain images were acquired with a quadrant detector-type scanning Kerr microscope. For the acquisition of all domain images a $\times 20$ objective was used, except for the images in Fig. 6, for which a $\times 50$ objective was used. Further details of the scanning Kerr microscope can be found in Ref. 19. If not mentioned otherwise, the hysteresis loops and the images shown here represent the magnetization component parallel to the applied field $M_{\parallel}$. In some cases the magnetization component $M_{\perp}$ perpendicular to the applied field is also of interest.

III. RESULTS

A. Hysteresis loops

Continuous film. The magnetization reversal in the Fe/GaAs(001) wires is discussed here for the case where the external field is applied parallel to the long and the short wire axes which are both hard magnetocrystalline anisotropy axes. The reversal for this field orientation will be summarized first for the continuous films. Further details of the reversal in continuous films, including the various domain formation, can be found in Refs. 12, 19, and 20.

As a result of the fourfold symmetry, the magnetization reversal as a function of an applied magnetic field takes place by a two-jump switching process.[12] The subsequent changes in the orientation of the magnetization during the reversal are indicated by the reversal steps (i)–(iv) in Fig. 2(a). The coordinate system in Fig. 2(a) defines the relative orientation between the crystallographic axes and the magnetocrystalline easy (EA) and hard (HA) anisotropy axes, as well as the direction of the initially applied field $H_{\rm init}$ and the reverse applied field $H_{\rm rev}$. Saturating the film into the initial field direction $H_{\rm init}$, the film is in a single-domain state with the magnetization aligned parallel to $H_{\rm init}$. On reducing the strength of the applied field, the magnetization coherently rotates from the initial field direction $H_{\rm init}$ to the nearest easy axis, e.g., the [100] direction, see step (i) in Fig. 2(a). On further reducing and reversing the applied field, the magnetization jumps discontinuously and irreversibly[12] from the single-domain state [100] into the single-domain state [010] at a critical field H_{c1},[21] as is indicated by step (ii) in Fig. 2(a). Increasing the reverse field to the critical field H_{c2}, the magnetization jumps a second time discontinuously and irreversibly from the [010] to the [100] direction,[12] [step (iii)] and finally rotates coherently into the reverse field direction $H_{\rm rev}$ [step (iv)]. Of particular note is the strict initial sense of rotation for this two-jump switching process[12] which is determined by the direction of the applied field with respect to the easy and hard anisotropy axes. For the example in Fig. 2(a) the initial sense of rotation is clockwise as long as the field is applied along a direction inbetween the [110] and [100] direction. This strict initial sense of rotation, which includes the two irreversible jumps and follows the sense of rotation of step (i), is of importance for the understanding of the domain growth processes in the wires.

Typical hysteresis loops for a continuous Fe/GaAs(001) film showing the characteristic two jumps at H_{c1} and H_{c2} are given in Figs. 2(b) and 2(c) for $H_{\rm init}\|$ [100] EA and for $H_{\rm init}\|$ [110] HA, respectively. If the field is applied parallel to one of the easy axes, the two critical fields H_{c1} and H_{c2} are separated by only a small field range 3–5 G.[12] For fields applied close to the hard axis ($\pm 5°$), the two critical fields are well separated (200–550 G).[12]

Wires. The corresponding averaged hysteresis loops for the wires are shown in Fig. 3 (Ref. 22) for the field aligned parallel to (a) the long wire axis or easy shape (ES) axis (dotted line) and (b) the short wire axis or hard shape (HS) axis (full line). Here easy shape and hard shape denote the fact that average demagnetization fields are much smaller for

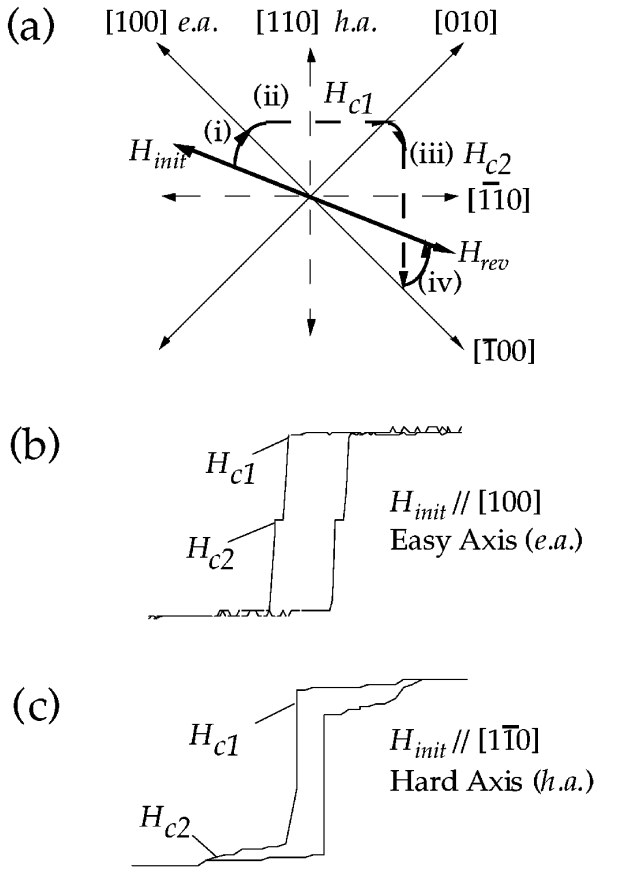

FIG. 2. (a) Orientation of the fourfold in-plane anisotropy axes relative to the crystallographic axes for Fe/GaAs(001) thin films. The easy anisotropy axes are parallel to ⟨100⟩ and the hard anisotropy axes parallel to ⟨110⟩. The dotted lines as well as the roman numbers (i)–(iv) are a guide for the subsequent steps in the magnetization reversal process. They indicate the changes in the direction of the magnetization on reversing an applied field from the initial field direction $H_{\rm init}$ into the reverse field direction $H_{\rm rev}$. The rounded parts correspond to a coherent rotation process [steps (i) and (iv)] and the straight parts to the discontinuous jumps between the easy axes [100] and [010] at H_{c1} and between [010] and [100] at H_{c2} [steps (ii) and (iii)]. (b) Typical averaged hysteresis loop for the magnetization component $M_{\|}$ for a continuous Fe/GaAs(001) thin film and for an initial field applied parallel to an easy magnetocrystalline anisotropy axis, e.g., [100]. (c) Typical averaged hystersis loop for the magnetization component $M_{\|}$ for a continuous Fe/GaAs(001) thin film and for an initial field applied parallel to a hard anisotropy axis, e.g., [110].

the long wire axis due to the large aspect ratio of l/w, although these average demagnetization fields play a negligible role for the reversal. Since the easy shape and hard shape anisotropy axes are both hard magnetocrystalline anisotropy axes, four different situations for the irreversible jumps at the two critical fields H_{c1} and H_{c2} can be distinguished: $H_{c1}^{\rm HS}$, $H_{c2}^{\rm HS}$, $H_{c1}^{\rm ES}$, and $H_{c2}^{\rm ES}$, where, e.g., $H_{c1}^{\rm HS}$ refers to the situation where the field is applied along the short or hard shape (HS) wire axis and the switching process at the first critical field H_{c1} is considered.

Both loops in Fig. 3 are very similar to the one of the continuous film shown in Fig. 2(c), confirming that the two-jump switching process, characteristic for fourfold anisotropic films, is not substantially altered in the wires. However, slight deviations between the HS and ES loops are evident. These deviations display an interesting symmetrical relationship at the two critical fields: at H_{c1} the magnetization $M_{\|}$ of the HS loop is more reduced from the saturation value and the loop is more rounded as compared to the ES loop, which is squarer at H_{c1}, whereas at H_{c2} the magnetization $M_{\|}$ of the ES loop is more reduced and the loop is more rounded as compared to the HS loop at H_{c2}.

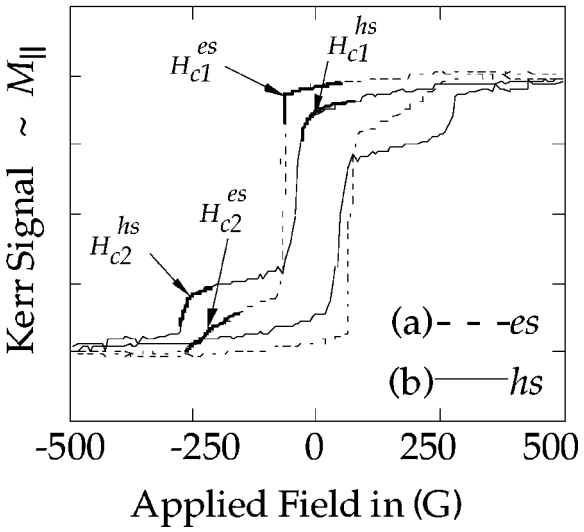

FIG. 3. Averaged hysteresis loops for a wire array of epitaxial Fe/GaAs(001) ($t=300$ Å, $l=500$ μm, $w=15$ μm, $s=22$ μm) for the two field orientations (a) parallel to the long wire axis (ES), dotted line, and (b) parallel to the short wire axis (HS), full line. The discontinuous and irreversible magnetization changes at the four different critical fields $H_{c1}^{\rm HS}$, $H_{c2}^{\rm HS}$, $H_{c1}^{\rm ES}$, and $H_{c2}^{\rm ES}$ are marked.

B. Domain images

Continuous film. The average demagnetization fields in continuous in-plane magnetized films are negligible and no remanent domain structure develops. However, domains nucleate and grow via domain-wall motion during the magnetization reversal at the two critical fields H_{c1} and H_{c2}. This domain process is responsible for the discontinuous and irreversible jumps seen in the average hysteresis loops. The developing domain structure and the orientation of the magnetization inside the domains reflect the fourfold symmetry but depend in detail on the orientation of the applied field with respect to the magnetocrystalline anisotropy axes. For fields applied parallel to an easy magnetocrystalline anisotropy axis, a checkerboard-type domain structure with all four magnetization orientations may develop.[19,20] In contrast, for fields applied parallel to one of the hard anisotropy axes, domains with only two magnetization orientations coexist. A typical example for the domain structure mediating the irreversible jump from the [100] direction to the [010] direction at H_{c1} in the continuous film is shown in Fig. 4. Only domains with orientations of the magnetization parallel to [100] and [010] are involved, separated by walls ideally aligned parallel to [110] which is a hard anisotropy axis, compare Fig. 2(a). Usually pinning obstructs a straight alignment of these walls as can be seen in Fig. 4. A similar domain structure develops for the reversal at H_{c2} where now domains are

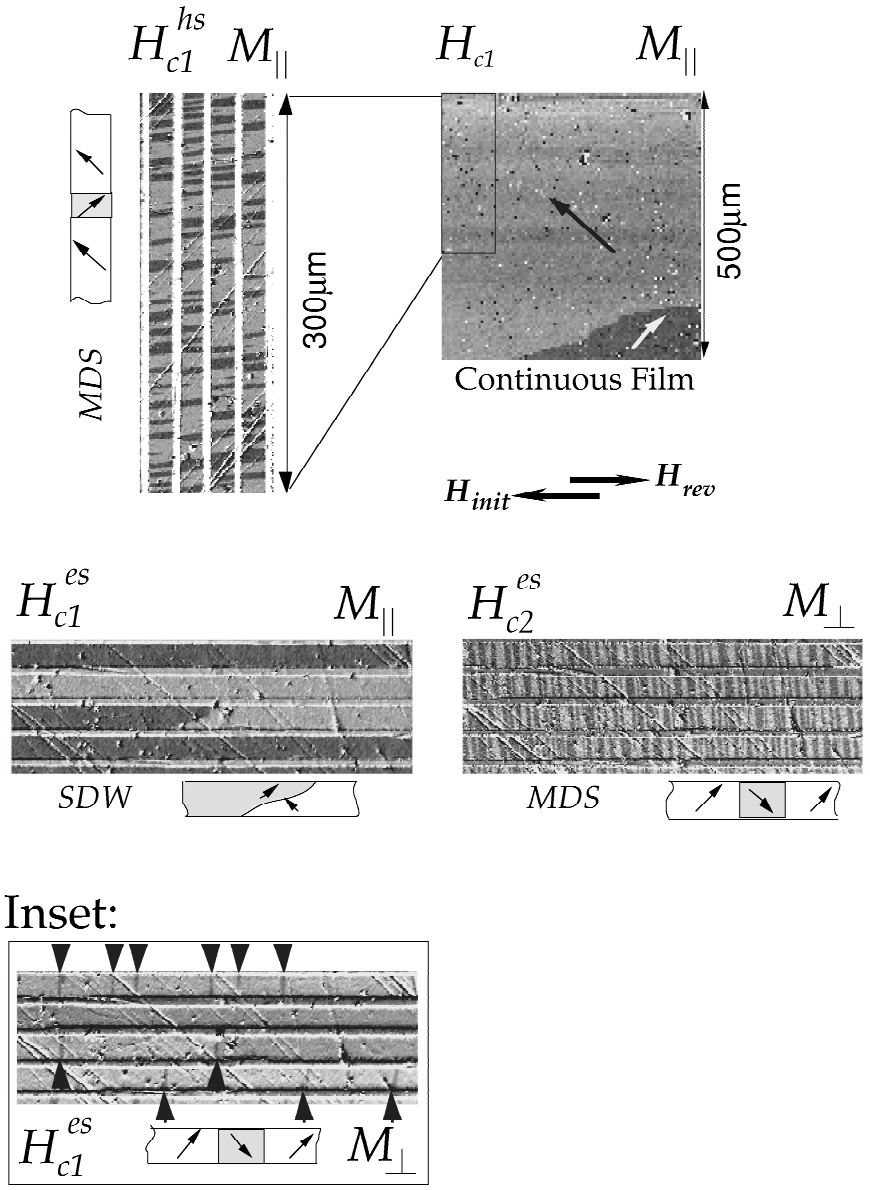

FIG. 4. Domain patterns developing in epitaxial Fe/GaAs(001) wires ($t=300$ Å, $l=500$ μm, $w=15$ μm, $s=8$ μm) at the three critical fields H_{c1}^{HS}, H_{c1}^{ES}, and H_{c2}^{ES}, as well as the domain pattern developing in the continuous film at H_{c1}. The wire domain images are taken on the identical sample areas. The adjacent schematics explain the orientation of the magnetization inside the domains. The contrast in the H_{c1}^{HS}, H_{c1}^{ES} images is due to changes in the magnetization component parallel to the applied field $M_{\parallel}$ and in the H_{c2}^{ES} case due to changes in the magnetization component $M_{\perp}$ perpendicular to the applied field. The inset shows the $M_{\perp}$ domain image for the H_{c1}^{ES} case complementing the $M_{\parallel}$ image above.

involved with an alignment of the magnetization parallel to the [010] and [100] directions and domain walls parallel to [100],[20] compare Fig. 2(a).

Wires. In Fig. 4 the domain structures in the wires, which develop at the critical fields H_{c1}^{HS}, H_{c1}^{ES}, H_{c2}^{ES}, are compared with the one which develops in the continuous film at the critical field H_{c1} during hard axis reversal. The imaged area for the wires is 100 μm$\times$300 μm containing four single wires. The equivalent size of this region is outlined in the 500 μm$\times$500 μm area of the continuous film in order to emphasize the different sizes of the domains. The continuous film constitutes a different area but is otherwise the identical film from which the wires were patterned. For all domain patterns, the light areas in the images correspond to the unswitched domains and the dark areas to the switched domains. Note that in Fig. 4 the orientation of the applied field is fixed for all domain images (as is the case in the experiment) and consequently in the HS configuration the long wire axes appear vertically and in the ES configuration they appear horizontally.

From Fig. 4 it is seen that different domain structures occur depending on the lateral film sizes as well as on the field orientation. Whereas in the continuous film a large domain sweeps through the film, the domains in the wires are much smaller in size. Furthermore, two distinct domain patterns can be distinguished for the wires which are referred to

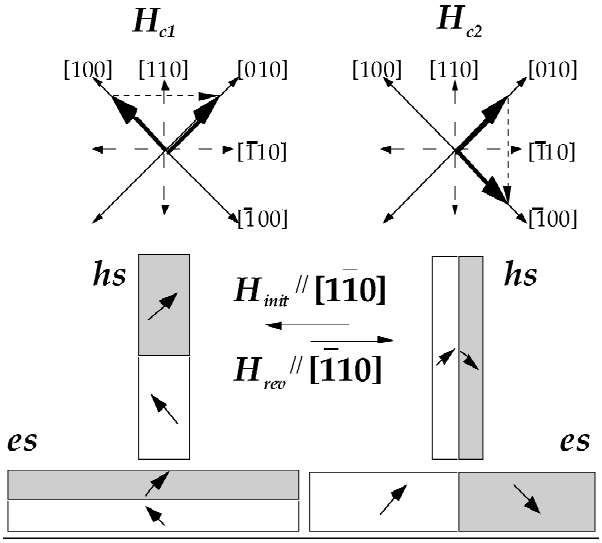

FIG. 5. Schematic depicting the symmetric relationship for the orientation of the magnetization inside the domains as well as the orientation of the domain walls relative to the wire edges at the two critical fields H_{c1} and H_{c2} and for the two field orientations $H\|$ES and $H\|$HS wire axis.

as (i) a multidomain structure (MDS), which develops at the critical fields H_{c1}^{HS} and H_{c2}^{ES} as shown in Fig. 4 and (ii) a single domain wall (SDW), which develops at the critical field H_{c1}^{ES} as shown in Fig. 4.

The same symmetry as was mentioned for the hysteresis loops in Fig. 3 is observed for the domains developing at the critical fields H_{c1}^{HS} and H_{c2}^{ES}: in both cases a MDS develops. The corresponding image of the domain structure developing at the critical field H_{c2}^{HS} which would complement the one developing at H_{c1}^{ES} is not available; however from the loop symmetry in Fig. 3 it is concluded that in both cases a SDW develops.

IV. DISCUSSION

A. Symmetry of the loops and domain images

The symmetry observed in the loops and the domain images at the critical fields H_{c1}^{HS} and H_{c2}^{ES}, as well as the symmetry observed in the loops at the critical fields H_{c1}^{ES} and H_{c2}^{HS} is in its basic essence a manifestation of the fourfold magnetocrystalline anisotropy or, alternatively expressed, serves as a demonstration of the underlying symmetry of this anisotropy. This can be seen by the following argument. Consider Fig. 2(a) where a switching [100] and [010] at H_{c1} and from [010] to [100] at H_{c2} is shown. The corresponding domains which mediate this switching are separated by domain walls which are aligned parallel to the [110] axis at H_{c1} and the [110] axis at H_{c2}, respectively.[20] According to this domain and domain-wall arrangement, the expected orientation of the magnetization inside the domains as well as the orientation of the domain walls relative to the wire edges can be derived for all four critical fields: H_{c1}^{HS}, H_{c2}^{ES}, H_{c1}^{ES}, and H_{c2}^{HS}. These expected configurations are shown schematically in Fig. 5. Note that here, as in Fig. 4, the orientation of the applied field is fixed and the wires are rotated such that in the displays of Figs. 4 and 5 the long wire axis is either vertically (HS) or horizontally (ES) aligned.

As is evident from Fig. 5, the expected wall orientations relative to the wire edges show the same symmetrical relationship as the loops in Fig. 3 and the domain images in Fig. 4. At the two critical fields H_{c1}^{HS} and H_{c2}^{ES} (rounded loop sections and MDS) the domain walls run across the short wire axis. Similarly, at the two critical fields H_{c2}^{HS} and H_{c1}^{ES} (squarer loop sections and SDW) domain walls are involved which run parallel to the long wire axis.

Loops. The irreversible and discontinuous switching processes at the critical fields H_{c1} and H_{c2} are largely determined by the growth of domains via domain-wall motion.[12] It can therefore be understood that the relative orientation of the domain walls with respect to the wire edges may play a role for the reversal process. In this sense, the symmetry seen in Fig. 3 between the HS and ES loops and at the two critical fields H_{c1} and H_{c2} reflects the fact that similar domain and domain-wall configurations with respect to the wire edges are responsible for the magnetization reversal at the respective symmetrical critical fields. However, the details of the shapes of the hysteresis loop, namely the rounding and the squareness, cannot be explained with this symmetry argument and will be further analyzed below.

Domains. A comparison of Fig. 5 with Fig. 4 reveals that the observed wall orientations separating domains which develop at the critical fields H_{c1}^{HS} and H_{c2}^{ES} follow the anticipated orientation with walls running parallel to the short wire axis. This is not obvious for the domain structure developing at H_{c1}^{ES}. Here the domains are observed to propagate from the left to the right in the image of Fig. 4 with walls running diagonally through the wire. Higher-resolution images, such as given in Fig. 6, show that some sections of this wall front (lower left) approach the anticipated alignment shown schematically in Fig. 5 with walls parallel to the long wire axis. Thus, there is a tendency towards the ideal wall alignment, but for reasons discussed later this is not fully achieved.

B. Anisotropic domain pattern

While the above argument explains the relative wall orientations and the occurrence of a symmetrical relationship for the domain patterns, it is not intuitively obvious what the driving mechanism is for the two very different domain patterns: (i) the MDS, in which a high nucleation rate predominates with a low domain growth rate and (ii) the SDW, with a low nucleation rate but a high domain growth rate. To be more specific, the following two questions need to be considered: (1) why is in case (i) the growth of a single domain from a short wire edge not as likely as in the case (ii) and (2) why do, in case (ii), more domains not nucleate? The answer to these questions lies in a combination of three effects: (a) local edge dipolar fields, (b) the strict initial sense of rotation of the magnetization during the reversal in fourfold anisotropic films, and (c) the anisotropic finite extensions of the wires. These effects are discussed in the following.

The reversal in the fourfold anisotropic Fe(001) films is characterized by a strict rotation sense of the magnetization, with the exception for fields applied precisely along the easy and hard anisotropy axes.[23] Upon reducing the applied field

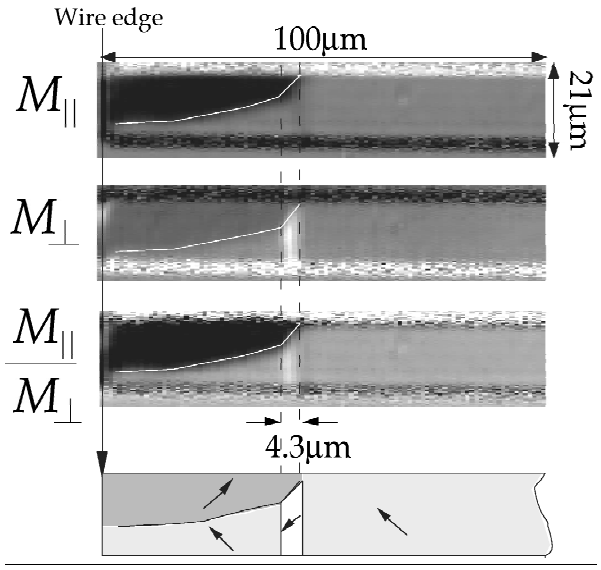

FIG. 6. Higher-resolution domain image (21 μm×100 μm) showing a SDW at the critical field H_{c1}^{ES}, which spreads from the left wire edge. The lower left section of the wall reaches nearly its ideal orientation which is parallel to the long wire edge (see Fig. 5). The upper right wall section is strongly distorted due to pinning and causes a small vertical domain to nucleate underneath. This vertical domain is only visible in the $M_{\perp}$ domain image. To emphasize the relation between the distorted wall front and the small vertical domain, an image displaying the ratio $M_{\parallel}/M_{\perp}$ is also shown. The schematic underneath indicates the orientation of the magnetization inside each domain.

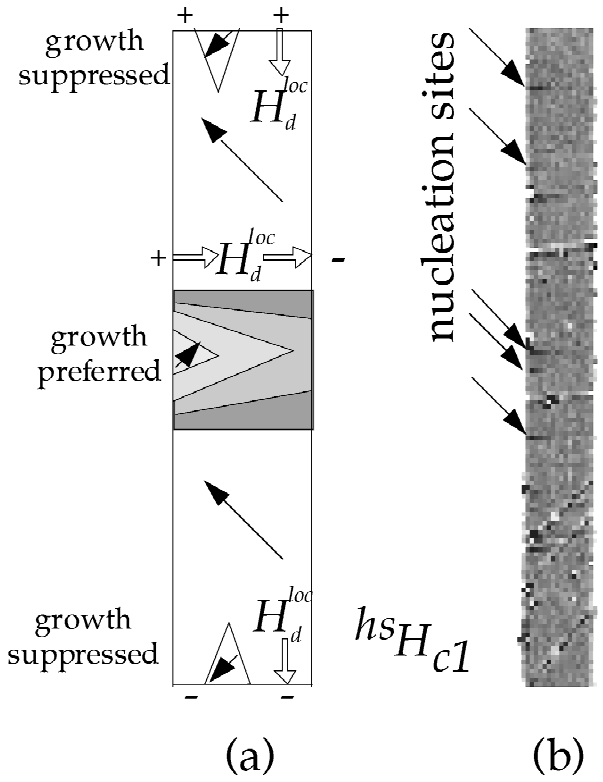

FIG. 7. (a) Schematic demonstrating the suppression and preferential growth of the edge domains at the critical field H_{c1}^{HS}. The charges alongside the edges are indicated by the ''+'' and ''−'' and the resulting local dipolar fields are indicated by the double arrow. (b) Enlarged section of a domain image showing edge domains growing from the long wire edge at the critical field H_{c1}^{HS}.

from the saturation field value, the magnetization rotates first coherently from the initial field direction into the nearest easy axis, compare Fig. 2(a). This initial rotation defines at the same time the rotation sense of the two irreversible jumps and is determined by the applied field direction. For the example in Fig. 2(a) this rotation sense is clockwise and in this case a counterclockwise jump from, e.g., [001] to [010], at H_{c1} is energetically less favorable.

Upon rotation of the magnetization from the initial field direction (parallel to a hard anisotropy axis) into the easy axis, charges build up along all four wire edges due to the 45° orientation of the easy axis relative to the wire edges. As is described in Sec. IV E, local dipolar fields arising from those charges will give rise to the nucleation of small edge domains in the vicinity of both the long and the short wire edges. In Fig. 7(a) these edge domains are schematically shown for a configuration corresponding to the critical field H_{c1}^{HS}. As these local edge dipolar fields superimpose onto the externally applied field, the magnetization switching inside the edge domains does not necessarily follow the rotation sense of the bulk of the wire. For the example in Fig. 7(a) this means that the magnetization switching inside the domains at the long wire edge follows the ''bulk'' rotation sense, whereas along the short wire edge it opposes the ''bulk'' rotation sense. A growth of the domains from the short wire edge would therefore require a switching of the magnetization of a large wire volume into an energetically less favorable direction. These domains are therefore most likely suppressed. The initial nucleation of edge domains cannot be made visible with the Kerr microscope due to its lower resolution, however Lorentz microscopy on similar structures confirms this nucleation process.[24] Upon increasing a reverse field these domains grow and also become visible in the Kerr image as shown in Fig. 7(b) where small domains expand from the long wire edge.

In summary, edge dipolar fields cause the nucleation of small edge domains. Due to the strict initial sense of rotation in fourfold anisotropic thin films only those edge domains nucleating along the long wire edge will grow preferentially at the critical fields H_{c1}^{HS} and H_{c2}^{ES} and correspondingly only those edge domains nucleating along the short wire edge will grow preferentially at the critical fields H_{c2}^{HS} and H_{c1}^{ES}.

This suppression and preferential growth of edge domains from only the short or long wire edge is a direct consequence of the edge dipolar fields and the fourfold anisotropy, but is independent of the anisotropic shape of the wires. A similar preferential growth is also observed for the domains in small Fe/GaAs(001) square elements with equal edge lengths.[9,19] Only the further evolution of these edge domains is influenced by the anisotropic and finite wire dimensions (500 μm vs 15 μm for the long vs short wire axis) resulting in the two domain patterns MDS and SDW. First, because of the large aspect radio l/w, the long wire edge offers many more nucleation sites than the short wire edge. In addition, the domains nucleating at the long edge need to expand only over a distance of 15 μm before they reach the opposite wire edge. Thus before these ''stripe'' domains begin to further expand in the direction of the long wire axis, many domains

have developed. Also it has to be assumed that the edges are not perfectly smooth and provide a very effective pinning mechanism for such short walls of only 15 μm length and thus prevent an expansion of the walls along the wire. Hence, at the two critical fields, H_{c1}^{HS} and H_{c2}^{ES}, the reversal is dominated by domain nucleation leading to the multidomain structure. In contrast to this, at the two critical fields H_{c2}^{HS} and H_{c1}^{ES}, where domains grow from the short wire edge, only a few domains can nucleate which, in turn, probably merge together quickly to form a single domain which subsequently spreads along the long wire axis as the reverse field is increased. As this domain has to expand over a long distance (500 μm) before it reaches the opposite wire edge, a complete straightening of its wall front is restricted. Thus the ideal wall configuration shown in Fig. 5 cannot be reached leaving diagonally stretched walls as seen in Figs. 4 and 6.

C. Anisotropy of the loops

While the symmetry argument illustrated in Fig. 5 explains the occurence of a symmetrical relationship for the shapes of the hysteresis loops in Fig. 3, an explanation for the fact that in one situation the loops are squarer and in the other more rounded cannot be derived. One might argue that short domain walls, such as occur at the critical fields H_{c1}^{HS}, H_{c2}^{ES}, will be pinned much more effectively as similar pinning sites act over a very short distance. This, however, would mainly influence the value of the critical field and less the shape of the loop in terms of squareness and rounding. Generally, for samples with large demagnetization shape anisotropies, the hysteresis loops $M_{\|}$ vs H_a (=applied field) are sheared due to the *average* dipolar (demagnetization) field $H_d^{av}=N\cdot M_s$,[25] with N the demagnetization factor. In the present case the rounding of the loops in Fig. 3 can be interpreted similarly as being due to the *local* edge dipolar fields. As was already mentioned above, edge domains nucleate in a small region δ in the vicinity of the edges. These edge domains lead to a reduction of the average magnetization $M_{\|}$ from the saturation value as measured, e.g., by MOKE. The different amount of rounding in the hysteresis loops indicates therefore a different degree of edge domain nucleation. Because the domain growth is anisotropic with respect to the wire edges and because the total length of the long wire edges is much larger than the short wire edge, the number of initially nucleated domains in the vicinity of the edges is much larger for the MDS than for the SDW structure. Hence, the magnetization is more reduced and the loops are more rounded at the critical fields H_{c1}^{HS} and H_{c2}^{ES}, where a MDS develops, as compared to the critical fields H_{c2}^{HS} and H_{c1}^{ES}, where a SDW develops.

D. Wires: Visibility of pinning sites

To complete the description of the domain evolution in the wires, an additional unexpected local dipolar field effect is mentioned briefly which occurs only when a SDW structure develops. In Fig. 4 the different domain states developing at the critical field H_{c1}^{ES} are shown for four adjacent wires. From this image three different snapshots of the domain evolution can be deduced; fully switched (top and bottom), fully unswitched (second from top), and half-switched–half-unswitched (second from bottom). A closer scan of the area around the domain-wall front such as in the half-switched wire is shown in Fig. 6 for both magnetization components $M_{\|}$ and $M_{\perp}$. The interpretation of the domain structure is indicated by the schematic underneath. Due to pinning at imperfections, the single domain-wall front, which spreads along the long wire axis as the reverse field is increased, distorts and builds up charges. Underneath those sections of the domain-wall front which are distorted by $\approx$45° with respect to the ideal wall orientation (compare Fig. 5) a small vertical domain of a few μm in width nucleates inside the unswitched domain. This vertical domain is visible in the $M_{\perp}$ domain image of Fig. 6. The orientation of the magnetization in this vertical domain is such that is shares a 180° wall with the switched domain. Upon further increasing the reverse field, the single domain-wall front depins, sweeps across the newly nucleated vertical domain, and spreads further along the wire. The small vertical domain however remains, reversing its $M_{\|}$ component when the SDW sweeps across the expanding across the full wire width. The persistence of these vertical domains after the SDW has spread through is evident from the inset in Fig. 4 which shows the $M_{\perp}$ image of the domains developing at the critical field H_{c1}^{ES}. The second wire from the top, which is unswitched, does not contain any vertical domains, whereas in the fully switched top and bottom wire small vertical domains show up at those positions where the motion of the single domain wall front has been halted at a pinning site. These positions are indicated by arrows. Hence, these vertical domains can be interpreted as ''fingerprints'' of the SDW pinning sites, or in other words, the nucleation of the vertical domains provide a mechanism with which to make the SDW pinning sites visible.

A final note is devoted to the nucleation process of the small vertical domain, which results from pinned and distorted single domain-wall fronts. This nucleation process is very similar to the one responsible for the development of checkerboard-type domains[19] during easy axis reversal in these fourfold Fe thin films. Domain propagation occurs here not only through wall expansion, but also through nucleation of domains at expanding distorted wall fronts. This demonstrates the importance of local dipolar fields for the reversal process which may influence the value of the critical fields.

E. Comparison to other small magnetic film elements

The micron-sized dimensions of the magnetic Fe(001) wires lead to a small but appreciable *macroscopic* (average) dipolar field H_d^{av} inside the wires oriented across the wire width. For the Fe/GaAs(001) wires, this average dipolar field can be estimated from the demagnetization field of a homogeneously magnetized ellipsoid of equivalent dimensions by $H_d^{av}=0.7\times M_s\times t/w$. Here the factor 0.7 takes into account that the easy axis of magnetization is aligned at 45° with respect to the wire edges, as illustrated in Fig. 1(b). This average dipolar field amounts to a value of $H_d^{av}\approx 30$ Oe for the wire dimensions given in Sec. II. It is much larger than the average dipolar field oriented along the long wire axis with $H_d^{av}\approx w/l\times 30$ Oe$=0.9$ Oe. As the anisotropy field $H_{K_1}=550$ Oe in Fe(001) is much stronger than these dipo-

lar fields H_d^{av}, the direction of the magnetization is locked through the anisotropy. The spins are not free to rotate into their resulting Maxwell field (applied plus dipolar) direction as is described for low anisotropic materials.[26] Therefore, in this configuration of the Fe wires, a substantial influence of the average dipolar fields on the remanent magnetization distribution is not expected. The 15-μm-wide Fe wire elements are found to be macroscopically in a single domain state at zero applied field. This is in contrast to the variety of remanent domain structures observed in small Permalloy film elements[27] having comparable sample dimensions.

The above estimates for H_d^{av} lead to the conclusion that the dipolar fields arising from the wire edges do not play a significant role for the magnetization distribution or the magnetization reversal process. However, the idealization of the wires as homogeneously magnetized ellipsoids is not adequate, as the wires have rectangular cross sections with sharp and well-defined edges. Hence, the dipolar field is not homogeneous and depends on the local position x, falling off as $(1/x)$, where x is the distance from the wire edge towards the center of the wire. In the center, the local dipolar field has a value of $H_d^{loc} \approx 20$ Oe which is lower than the average dipolar field $H_d^{av} \approx 30$ Oe. But in the vicinity of the edges, the local dipolar field can rise to a substantial value and is larger than the anisotropy field ≈ 550 Oe at a distance of $\delta < 0.1$ μm from the wire edge.[19] In this region δ, small domains may nucleate with an orientation of the magnetization determined by the competition between the local edge dipolar field and the anisotropy field. Such small domains cannot be made visible with the scanning Kerr microscope used here, but were observed in similar Fe/GaAs(001) square elements by Lorentz microscopy.[9] Triangular-shaped edge domains were seen to persist in an applied field nearly up to the anisotropy field.[24]

It is worthwhile to compare the nucleation of these triangular edge domains with the remanent domain configuration observed in soft Permalloy film elements of comparable sample dimensions. Here, too, the dipolar fields arising at the edges lead to the nucleation of domains whose orientation follows the local effective field (Maxwell plus anisotropy field).[26] The corresponding domains carry the charges away from the edges into the volume, thus spreading the charges over larger areas and effectively diluting and weakening the edge dipolar fields. Due to the low anisotropy field in Permalloy, these dipolar fields, which are located at the domain walls, are still large enough to induce further domains until an equilibrium domain structure, such as the Landau-Lifshitz or the concertina structure[27] is reached. The difference for the case of the Fe/GaAs(001) elements is that, due to the much stronger fourfold anisotropy, the dipolar fields located at these submicron edge domain walls are too small to induce any further domains. Hence in this configuration the Fe wires are essentially in a single-domain state. The dimensions of the Fe elements would have to be reduced by another order of magnitude from those studied here for similar effects to take place.

However, as shown by Gu *et al.*,[9] a remanent domain structure can form in Fe(001) square film elements even for sample sizes as large as 12 μm. Although dipolar fields do not overcome the anisotropy energy barrier for a macroscopic volume of these small film elements, they can be strong enough to induce a domain-wall displacement given that the critical field (depinning field) is smaller than the local dipolar field.[9] Hence, once small edge domains nucleate, these edge domains can grow through wall displacement under the influence of their own dipolar field. Consequently one can distinguish two processes which lead to a remanent domain structure.

In contrast to the studies of the Fe square elements,[9] the wires studied here have depinning fields which are larger than the average dipolar fields. This is expressed by the relatively large reverse field that is needed to propagate the nucleated edge domains. The depinning field of the wires is observed to be 30–70 Oe, whereas the depinning field of the continuous film, from which the wires were patterned, is 10–16 Oe. This larger depinning field is attributed to less perfect and rough wire edges. Thus the Fe/GaAs(001) wires investigated here provide a complementary view on the evolution of the edge domains where pinning hinders a free expansion of the domain walls in its self-demagnetizing field. In other words, the domain growth in a reverse applied magnetic field described here can be understood as the ''slow motion'' process for the evolution of the remanent domains observed in Ref. 9.

V. SUMMARY

In summary, the magnetization reversal in micron-sized epitaxial Fe/GaAs(001) wires was investigated and it was shown that the two-step switching process is preserved but that the domain evolution is anisotropic. For the same critical fields, H_{c1} or H_{c2}, the developing domain pattern is dependent on the orientation of the applied field with respect to the long and the short wire axes, see Fig. 4. This anisotropy is a finite-size effect and only indirectly a dipolar (demagnetization) field effect. As in the wires, the ratio of the edges relative to the total wire volume is much larger as compared to the continuous film, the influence of the edges on the nucleation and growth of domains increases. This influence is particularly strong in the case where domain growth from the long wire edge is favored (MDS). In this case the domain pattern deviates strongly from the one seen in the continuous film. This is in contrast to the case where domain growth from the short wire edge is favored (SDW). Here the domain pattern is similar to the one in the continuous film and can even be seen as a small horizontal ''slice'' of the image shown in Fig. 4 for the continuous film. The reason for this similarity is that in both cases a single-domain front stretches out into a large film volume, whereas in the MDS the physical boundaries of the wire width hinder such a domain expansion.

The discussions here were mainly restricted to local dipolar fields in conjunction with the fourfold anisotropy and the finite extension of the wires. The edge quality plays only a secondary role and does not affect the initial edge domain nucleation. Thus the anisotropy in the subsequent domain evolution, leading to the two different domain patterns MDS and SDW, can be regarded as a general property of the domain reversal processes in micron-sized epitaxial Fe(001) wires with wire edges parallel to the hard magnetocrystalline anisotropy axes. In particular one may conclude that for a better edge quality with less pinning efficiency, a MDS may occur as a remanent domain structure due to wall displace-

ment in the self-demagnetization field, similarly to the domain structures observed in Fe/GaAs(001) square elements.[9] A remaining question is to what extent the rough and imperfect edges influence the number of the initially nucleated domains, which needs further investigation with samples of higher edge quality.

ACKNOWLEDGMENTS

The support of EPSRC, Newton Trust (Cambridge), and the European Human Capital and Mobility Program is gratefully acknowledged. We further thank Professor H. Almed for making available the microfabrication facilities.

*Also at Dept. of Physics, The Ohio State University, Columbus, Ohio 43210.

†Also at University of York, Department of Physics, Heslington, York Y01 5DD, UK.

[1] *Ultrathin Magnetic Structures*, edited by J. A. C. Bland and B. Heinrich (Springer-Verlag, Berlin, 1994), Vols. I and II.

[2] A. D. Kent, S. von Molnar, S. Gider, and D. D. Awschalom, J. Appl. Phys. **76**, 6656 (1994).

[3] S. Y. Chou, M. S. Wei, P. R. Krauss, and P. B. Fisher, J. Appl. Phys. **76**, 6673 (1994).

[4] D. D. Awschalom and D. P. DiVincenzo, Phys. Today **48** (4), 43 (1995).

[5] A. Moschel, R. A. Hyman, A. Zangwill, and M. D. Stiles, Phys. Rev. Lett. **77,** 3653 (1996).

[6] A. O. Adeyeye, J. A. C. Bland, C. Daboo, J. Lee, U. Ebels, and H. Ahmed, J. Appl. Phys. **79**, 6120 (1996).

[7] E. J. Ozimek and D. I. Paul, J. Appl. Phys. **55**, 2232 (1984).

[8] N. Smith, IEEE Trans. Magn. Mag. **23**, 259 (1987); N. Smith, J. Appl. Phys. **3**, 2932 (1988).

[9] E. Gu, E. Ahmad, S. J. Gray, C. Daboo, J. A. C. Bland, M. Brown, M. Rührig, A. J. McGibbon, and J. N. Chapman, Phys. Rev. Lett. **78**, 1158 (1997).

[10] C. Shearwood, S. J. Blundell, M. J. Baird, J. A. C. Bland, M. Gester, H. Ahmed, and H. P. Hughes, J. Appl. Phys. **75**, 5249 (1994).

[11] J. M. Florczak and E. D. Dahlberg, Phys. Rev. B **44**, 9338 (1991).

[12] C. Daboo, R. J. Hicken, E. Gu, M. Gester, S. J. Gray, D. E. P. Eley, E. Ahmed, J. A. C. Bland, R. Ploessl, and J. N. Chapman, Phys. Rev. B **51**, 15 964 (1995).

[13] M. Gester, C. Daboo, R. J. Hicken, S. J. Gray, A. Ercole, and J. A. C. Bland, J. Appl. Phys. **80**, 347 (1996).

[14] J. Chen and J. L. Erskine, Phys. Rev. Lett. **68**, 1212 (1992).

[15] R. P. Cowburn, S. J. Gray, J. Ferre, J. A. C. Bland, and J. Miltat, J. Appl. Phys. **78**, 7210 (1995).

[16] G. A. Prinz, Science **250**, 1092 (1990); G. A. Prinz, Phys. Today **48** (4), 58 (1995).

[17] M. Johnson, J. Magn. Magn. Mater. **156**, 321 (1996).

[18] A. O. Adeyeye, Ph. D. thesis, University of Cambridge, 1996.

[19] U. Ebels, Ph. D. thesis, University of Cambridge, 1995.

[20] E. Gu, J. A. C. Bland, C. Daboo, M. Gester, L. M. Brown, R. Ploessl, and J. N. Chapman, Phys. Rev. B **51**, 3596 (1995).

[21] For the sake of clarity, the notation of the two critical fields H_{c1} and H_{c2} is reversed from that in Ref. 12.

[22] The hysteresis loops displayed in Fig. 3 are slightly modified from the original ones given in Ref. 19 in order to emphasize the symmetric relationship. The original hysteresis loops show a quadratic contribution to the Kerr effect $\propto M_s^2$, which emphasizes the jump at H_{c2} for one half cycle, but suppresses the jump in the other half cycle. As this is a purely optical effect and has no consequence on the characteristic loop shape itself, it was chosen to display only one half cycle of the original hysteresis loops in repetition for both half cycles. The actual change in the magnetization at the second jump is therefore only half the size of that displayed in Fig. 3.

[23] U. Ebels, M. Gester, C. Daboo, and J. A. C. Bland, Thin Solid Films **275**, 172 (1996).

[24] E. Gu (private communication).

[25] S. Chikazumi, *Physics of Magnetism* (Wiley, New York, 1964).

[26] F. A. N. Van der Voort and H. A. M. Van den Berg, IEEE Trans. Magn. Mag. **23**, 250 (1987).

[27] G. W. Garnett and W. D. Corner, J. Magn. Magn. Mater. **30**, 11 (1982).